PHYSICAL REVIEW B VOLUME 18, NUMBER 6 15 SEPTEMBER 1978

Coherent-potential-approximation calculations for PdH_x

D. A. Papaconstantopoulos and B. M. Klein
Naval Research Laboratory, Washington, D. C. 20375

J. S. Faulkner
Oak Ridge National Laboratory, Oak Ridge, Tennessee 37830

L. L. Boyer
Naval Research Laboratory, Washington, D. C. 20375

(Received 8 May 1978)

The angular-momentum components of the density of states (DOS) for substoichiometric PdH_x were calculated by the coherent-potential approximation (CPA). A tight-binding form of the CPA was used, based on a Slater-Koster fit to first-principles APW calculations. The CPA DOS's have been used to calculate the electron-phonon interaction and superconducting transition temperatures as a function of hydrogen concentration x. The results are in good agreement with experiment and with previous calculations in which the rigid-band model was utilized. The CPA results for the electronic-specific-heat coefficient as a function of x are in excellent agreement with experiment while the results of the rigid-band model are not.

I. INTRODUCTION

A technique for calculating the electronic states of substoichiometric crystals based on the coherent-potential approximation (CPA),[1] was developed by Faulkner[2] and applied to PdH_x. The purpose of the present work is twofold: (a) to implement Faulkner's method utilizing a more sophisticated Slater-Koster Hamiltonian and to improve on some computational aspects of this method, and (b) to determine the electron-phonon interaction as a function of hydrogen concentration and compare the results with previous calculations[3,4] in which the rigid-band approximation was used.

In Sec. II we discuss the Slater-Koster interpolation scheme[5] and the way it has been applied to the present work. We emphasize the importance of fitting high bands in order to obtain the correct angular-momentum character of the site densities of states.

In Sec. III we briefly review Faulkner's CPA theory[2] of substoichiometric systems and present details on the computational procedure that we have followed.

In Sec. IV the results are presented and compared with experiment. We have obtained good agreement with photoemission,[6] specific-heat,[7] and superconductivity[8-11] measurements. We have also verified that the rigid-band model is a reliable approximation for obtaining the Fermi-level values of the densities of states as a function of hydrogen content, but it is unreliable for locating the position of the low-lying hydrogen-bonding states.

II. SLATER-KOSTER INTERPOLATION

The LCAO interpolation scheme of Slater and Koster[5] has been used extensively to generate the total density of states (DOS) from the energy bands for a given material. Connolly[12] has given a detailed account of the method for the bcc and CsCl structures, while Mattheiss,[13] Honig *et al.*,[14] and Schwarz[15] have applied it to the NaCl structure. Mattheiss[16] has also extended the method for more complicated structures such as the A-15 structure.

In the case of PdH the Slater-Koster scheme was first applied by Switendick,[17] who used a total of ten basis functions involving the s, p, and d orbitals of Pd and the s orbital of H. He fitted 46 APW energies at the Γ (0,0,0), Δ (0,4,0), X (0,8,0), Σ (4,4,0), W (4,8,0), and L (4,4,4) (in units of $\pi/4a$) points in the Brillouin zone, and used 29 parameters, three of which represented the overlap integrals between Pd and H orbitals as proposed by Mattheiss.[13]

Before we enter into a detailed discussion of our Slater-Koster calculations, we wish to first state what we believe is an important conclusion from our extensive study of this interpolation procedure. In order to obtain a reliable decomposition of the DOS into its angular momentum components we must achieve a consistency between the basis set used in our Slater-Koster matrix and the levels fitted from the first principles band calculation. For the particular case of PdH this means that since we have two sets of s orbitals (one for Pd and one for H) we must fit both the low bonding states and the states of s character above the Fermi level (see Fig. 1). In addition, since we have

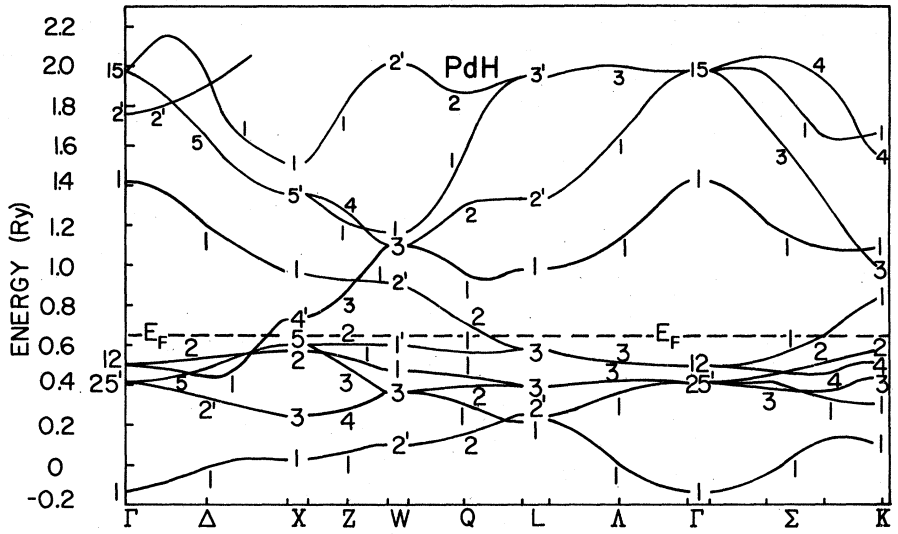

FIG. 1. Energy bands of stoichiometric PdH.

p orbitals in our basis set we must include in the fit p states which are high in energy (near Γ_{15} in Fig. 1).

We first applied the Slater-Koster method with the same basis functions used by Switendick but by also including third-neighbor interactions, which increased our parameters to 41. We then dropped the three overlap parameters and noticed no appreciable differences in our DOS results. In order to simplify the CPA calculations in the work presented here, we have formed Bloch sums from orthogonal atomic orbitals. We have not included any overlap integrals since they do not change the DOS by more than a few percent. The 38 interaction integrals for PdH, treated as parameters, are given in Table I together with the corresponding 32 parameters found from our pure Pd calculation. These parameters were determined by a nonlinear least-square procedure[18] after reducing the size of the 10×10 secular equation (9×9 for Pd) by symmetry. This reduction of the matrix size was accomplished by using the symmetrized linear combinations of spherical harmonics for the symmetry points and lines in

TABLE I. Slater-Koster parameters expressed in rydbergs. The abbreviations $d_1 \equiv x^2-y^2$ and $d_2 \equiv 3z^2-r^2$ are made.

	Pd–Pd Interactions Pure Pd	PdH		Pd–Pd Interactions Pure Pd	PdH
$E_{s_1,s_1}(000)$	0.9057	0.8031	$E_{d_2,d_2}(110)$	−0.0180	−0.0203
$E_{s_1,s_1}(110)$	−0.0822	−0.0749	$E_{d_1,d_1}(110)$	0.0313	0.0435
$E_{s_1,x_1}(110)$	0.0832	0.0663	$E_{s_1,s_1}(200)$	0.0074	−0.0012
$E_{s_1,xy}(110)$	0.0523	0.0449	$E_{s_1,x_1}(200)$	−0.0173	0.0161
$E_{s_1,d_2}(110)$	0.0218	0.0288	$E_{s_1,d_2}(002)$	−0.0122	−0.0453
$E_{x_1,x_1}(000)$	1.4450	1.3343	$E_{x_1,x_1}(200)$	−0.0130	−0.0045
$E_{x_1,x_1}(110)$	0.0823	0.0721	$E_{y_1,y_1}(200)$	0.0066	0.0025
$E_{x_1,x_1}(011)$	−0.0043	−0.0059	$E_{x_1,xy}(020)$	0.0003	0.0024
$E_{x_1,y_1}(110)$	0.1101	0.1073	$E_{z_1,d_2}(002)$	0.0028	−0.0389
$E_{x_1,xy}(110)$	−0.0515	−0.0251	$E_{xy,xy}(200)$	−0.0024	0.0001
$E_{x_1,xy}(011)$	0.0122	0.0269	$E_{xy,xy}(002)$	0.0006	0.0010
$E_{z_1,d_2}(011)$	0.0055	0.0062	$E_{d_2,d_2}(002)$	−0.0028	−0.0126
$E_{z_1,d_1}(011)$	0.0302	0.0420	$E_{d_1,d_1}(002)$	0.0000	−0.0033
$E_{xy,xy}(000)$	0.3883	0.4643		H–H Interactions	
$E_{xy,xy}(110)$	−0.0395	−0.0335	$E_{s_2,s_2}(000)$	···	1.0839
$E_{xy,xy}(011)$	0.0101	0.0080	$E_{s_2,s_2}(110)$	···	0.0208
$E_{xy,yz}(011)$	0.0119	0.0133	$E_{s_2,s_2}(200)$	···	0.0045
$E_{xy,d_2}(110)$	0.0192	0.0183		Pd–H Interactions	
$E_{d_2,d_2}(000)$	0.3538	0.4074	$E_{s_1,s_2}(100)$	···	−0.0384
			$E_{x_1,s_2}(100)$	···	0.1298
			$E_{d_2,s_2}(001)$	···	0.0005

the fcc Brillouin zone given by Cornwell.[19] We have fit 111 and 127 energy values from our band calculations[4] for Pd and PdH, respectively, at the following $\vec{k}$ points: Γ (0,0,0), Δ (0,2,0), Δ (0,4,0), Δ (0,6,0), X (0,8,0), Σ(2,2,0), Σ(4,4,0), K (6,6,0), Z (2,8,0), W (4,8,0), Λ (2,2,2), L (4,4,4), Q (4,6,2), (2,4,0), (2,6,0), (4,6,0), (2,4,2), (2,6,2), and (4,4,2), in units of $\pi/4a$. For PdH, we have used here the results from our calculation denoted by SC-A in Ref. 4. This calculation was performed self-consistently with lattice constant $a = 4.09$ Å, the $X\alpha$ values of exchange $\alpha_{Pd} = 0.702$, $\alpha_H = 0.777$, and included spin-independent relativistic effects. The results are shown in Fig. 1. A similar calculation[4] for Pd was also performed and used to evaluate the pure Pd Slater-Koster parameters. We have included in the fit for Pd, the first six bands, and also six energies from the seventh and eighth bands with s- or p-like character; and for PdH the first seven bands of Fig. 1 and six energies from the eighth and ninth bands having p-like character. We have excluded from the fit points of f-like character like the Γ_2' (see Fig. 1), since our Slater-Koster scheme does not treat f bands in its present form. As stated in the beginning of this section, in the course of this study we realized that the projected DOS are extremely sensitive to whether we successfully fit the high bands. That is, the l components of the DOS change dramatically upon including these bands. We came to the conclusion that one can reproduce an accurate total DOS (up to E_F) by fitting the first six bands, but it is necessary to include the seventh, and the eight or ninth bands, in order to obtain reliable angular-momentum-decomposed DOS. In Table II we give the rms fitting error per band for both the Pd and PdH calculations. It should be noted here that our rms error for the fifth and sixth bands, where E_F lies, is quite small. It could have been made even smaller if we had not included the high bands, but this would seriously alter the l character of the DOS as mentioned above. Having determined the Slater-Koster parameters we calculated the DOS by diagonalizing the 10×10 (9×9 for pure Pd) secular equation. To check the convergence of the DOS calculations we have plotted in Fig. 2 the total DOS, n_t, at E_F, as a function of the number of $\vec{k}$ points for a uniform mesh in the $\frac{1}{48}$th of the Brillouin zone. We note that satisfactory convergence is obtained when the DOS is computed from more than 2992 $\vec{k}$ points in the $\frac{1}{48}$th of the zone. We also observe from Fig. 2 that the results of the 770-$\vec{k}$-point mesh are very close to the converged results at E_F. This holds true for all energies near E_F. Since the CPA calculations described in Sec. III consume a very substantial amount of computer time, we performed our calculations on the 770 mesh and we estimate that our error does not exceed 2%.

TABLE II. rms error of the fit to the APW energies computed for 89 $\vec{k}$ points.

Band	rms error (Ry) Pd	PdH
1	0.007	0.021
2	0.007	0.017
3	0.014	0.021
4	0.011	0.009
5	0.006	0.007
6	0.013	0.007
7	0.030	0.015
8	0.055	0.058

The present Slater-Koster interpolation gives a fit to the APW bands which is more accurate than that used in Ref. 2. This is due to the fact that in Ref. 2 the two-center approximation was made and only 15 adjustable parameters were used.

The Slater-Koster total DOS agrees to within 2% with the DOS derived by the QUAD method in Ref. 4. A comparison of the l components of the DOS, n_l, is not possible since in Ref. 3 we obtained n_l within the muffin-tin spheres, while now the Slater-Koster method gives these quantities within the total unit cell.

III. CPA CALCULATIONS

The Slater-Koster Hamiltonian introduced in the previous section was used to solve the CPA equations. Since the details of this approach are given in Ref. 2, we will present here only the basic

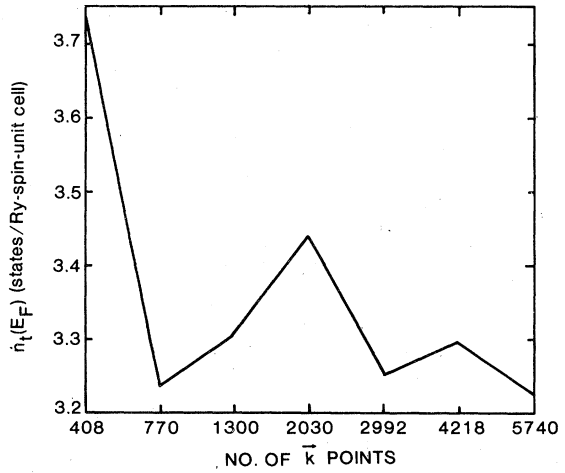

FIG. 2. Total density of states at the Fermi level plotted vs the number of $\vec{k}$ points in the $\frac{1}{48}$th of the Brillouin zone.

equations and then proceed to discuss certain computational aspects of this method. The form of the CPA used here is based on the assumption that the metal-ion sub-lattice is perfectly periodic, but the nonmetal sublattice can have vacant sites. The CPA leads to a periodic Hamiltonian H which has the property that quantities calculated from the Green's function,

$$G(z)=1/(z-H), \tag{1}$$

are good approximations to those that would be found from the actual nonperiodic Hamiltonian. The equation for an element of the Green's function is

$$G_{i,j}(\sigma,E)=\frac{1}{\Omega}\lim_{z\to E^+}\int d\vec{k}\,[z\Delta_{i,j}(\vec{k})-H_{i,j}(\vec{k},\sigma)]^{-1}, \tag{2}$$

where $\Delta_{i,j}(\vec{k})$ are the elements of the overlap matrix which we have set equal to unity, and

$$H_{i,j}(\vec{k},\sigma)=\begin{cases} H^0_{i,j}(\vec{k}) & \text{for } i,j=1,2,\ldots,10 \\ H^0_{i,j}(\vec{k})-E_{s_2,s_2}(000)+\sigma(E) & \text{for } i=j=10. \end{cases} \tag{3}$$

In this equation $H^0_{i,j}(\vec{k})$ are the matrix elements of the Slater-Koster Hamiltonian, and $E_{s_2,s_2}(000)$ is the hydrogen-hydrogen interaction parameter listed in Table I. The complex function $\sigma(E)$ is the CPA self-energy, which is determined by the equation

$$\sigma(E)=E_{s_2,s_2}(000)-C/G_{10,10}(\sigma,E), \tag{4}$$

where C is the concentration of vacancies. The element $G_{10,10}(\sigma,E)$ is a function of σ and we can solve Eqs. (2) and (4) by iteration. The DOS per spin is then determined from the following well-known expression:

$$n_t(E)=-\frac{1}{\pi}\lim_{z\to E^+}\mathrm{Im}[\mathrm{Tr}G(z)]\,. \tag{5}$$

By partitioning $G(z)$ we have calculated from expressions similar to Eq. (5) the decomposed densities of states which are plotted in Fig. 3.

In this model the electron is excluded from sites where there is a vacancy by setting the site energy $E^{\mathrm{vac}}_{s,s}(000)$ equal to infinity. For this reason the question of off-diagonal randomness never arises. Equations (2) and (4) are relatively easy to solve because the self-energy $\sigma(E)$ is a scalar. If it had been necessary to put higher angular-momentum states on the hydrogen sites, $\sigma(E)$ would be a matrix.

In calculating the CPA DOS as a function of hydrogen concentration x we have performed a weighted sum over 770 $\vec{k}$ points in the $\frac{1}{48}$th of the

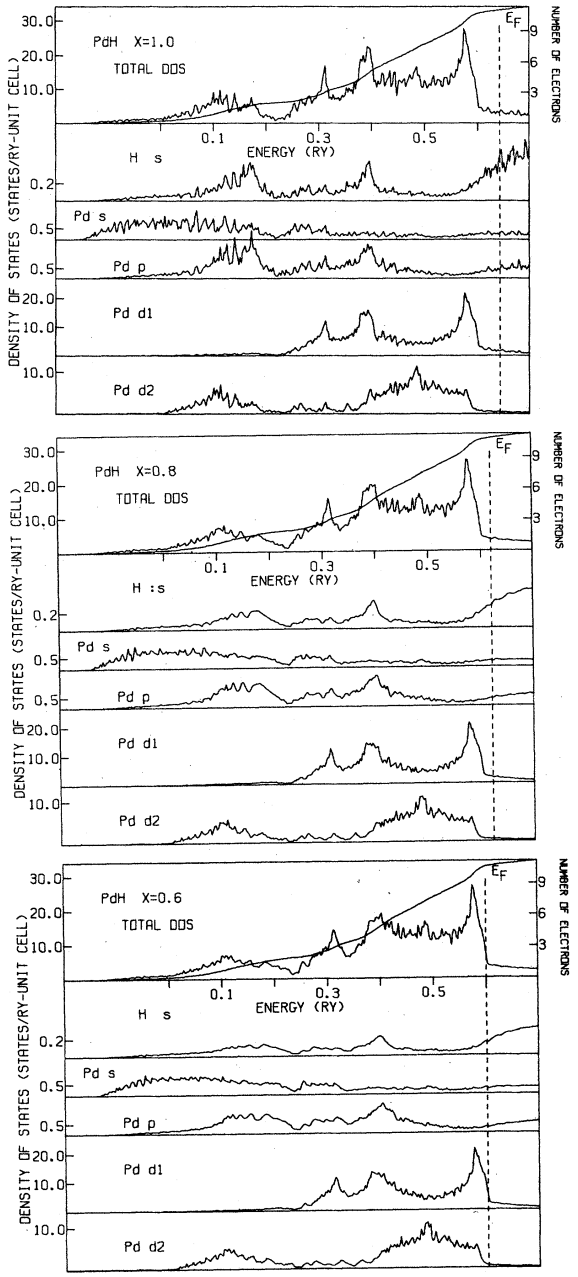

FIG. 3. Total and component densities of states plotted vs energy for three hydrogen concentrations $x=1.0$, 0.8, and 0.6.

Brillouin zone. As discussed in Sec. II an inspection of Fig. 2 shows that the 770-$\vec{k}$-point mesh gives results which are very close to the converged results of the 2992 $\vec{k}$ mesh. Also, setting the overlap matrix equal to unity makes the CPA calculations computationally more tractable with no significant loss of accuracy, as mentioned in Sec. II.

We have calculated the DOS for 360 values in the

range from −0.20 to 0.70 Ry so that our energy step is $\Delta E = 0.0025$ Ry. In the calculation of the DOS from Eq. (5) a small imaginary part ϵ must be added to the energy. The size of ΔE and the value of ϵ can cause serious convergence problems, as, strictly speaking, the results are independent of ϵ only in the limits that $\Delta E \to 0$ and the $\vec{k}$-space mesh used for the integrations becomes infinitely fine. We have checked the convergence of the DOS by varying the values of ϵ and ΔE. Comparing with the results of the straight Slater-Koster DOS at $x = 1.0$, we have concluded that convergence to within 2% on the 770-point mesh was achieved for $\epsilon = 0.001$ Ry and $\Delta E = 0.0025$ Ry.

IV. RESULTS

We have calculated the DOS of PdH_x for $x = 1.0$, 0.9, 0.8, 0.7, 0.6, 0.5, 0.4, 0.3, 0.2, 0.1, and 0.0. The results for $x = 1.0$, 0.8, and 0.6 are shown in Fig. 3, as we are primarily interested in the larger hydrogen concentrations. In Fig. 3, the symbols d_1 and d_2 indicate the Pd site DOS of t_{2g} and e_g, symmetry respectively. An inspection of this figure reveals that the center of gravity of the states with large hydrogen participation is essentially independent of hydrogen concentration. This is in agreement with the recent calculations of Gelatt *et al.*[20] in which the average-t-matrix approximation (ATA) was used. In Ref. 4 we argued for a linear shift of the low s band with x. This notion is not supported by the present calculations. A comparison of our CPA hydrogen-site DOS with the photoemission measurements of Eastman *et al.*[6] leads to good agreement. The experiment finds the hydrogen-induced states centered at 5.4 eV below E_F. Our calculations from Fig. 3 ($x = 0.6$) show the H-site DOS peaking at about 0.43 Ry or 5.9 eV below E_F.

In Fig. 4 we have plotted the value of the total DOS, n_t, at E_F versus x. We note that n_t is about constant in the region $0.8 < x < 1.0$, and it takes much higher values as the amount of hydrogen is reduced. It also approaches the palladium DOS limit for $x \to 0$.

In previous papers[3,4] we used the total and angular-momentum-decomposed DOS, within the rigid-band approximation (RBA), to obtain the electron-phonon interaction η and the superconducting transition temperature T_c as a function of x. Our results were in very good agreement with experiment and thus seemed to justify the applicability of the RBA on the PdH system. We had argued that the RBA is reliable when one utilizes DOS information which is obtained from a narrow energy range near E_F. Its validity can certainly be questioned away

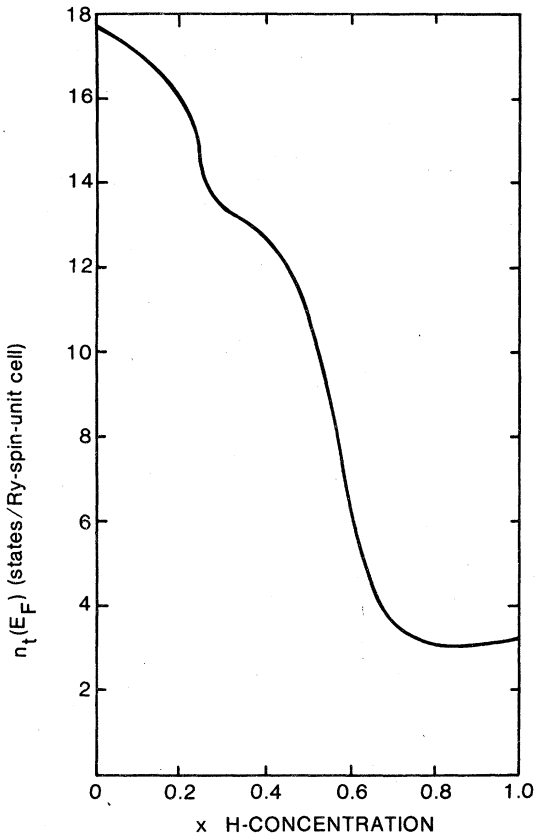

FIG. 4. Total density of states at the Fermi level plotted vs hydrogen concentration.

from E_F when one is interested, for example, in the position of the bonding states.

In Fig. 5 we have plotted the CPA values of the hydrogen s-like DOS n_{sH} at E_F as a function of x. We note that n_{sH} increases rapidly with x as it did for the RBA results. We have argued before[3,4] that the experimentally observed increase of T_c with x is mainly due to the increase of n_{sH} with x. The same conclusion can now be drawn from the CPA calculations.

In our previous work[3,4] we calculated η from the following formula due to Gaspari and Gyorffy,[21]

$$\eta_s = \frac{E_F}{\pi^2 n_t} \sum_{l=0}^{2} \frac{2(l+1)\sin^2(\delta_{l+1,s} - \delta_{l,s}) n_{l+1,s} n_{l,s}}{n^{(1)}_{l+1,s} n^{(1)}_{l,s}}, \tag{6}$$

where the index s stands for Pd or H, $\delta_{l,s}$ are the scattering phase shifts evaluated at E_F and at the muffin-tin radii, $n_{l,s}$ are the DOS within the muffin-tin spheres, and $n^{(1)}_{l,s}$ the "free scatterer" DOS as defined in Ref. 21. This theory of Gaspari and Gyorffy is formulated within the muffin-tin approximation and utilizes the l components of the DOS within

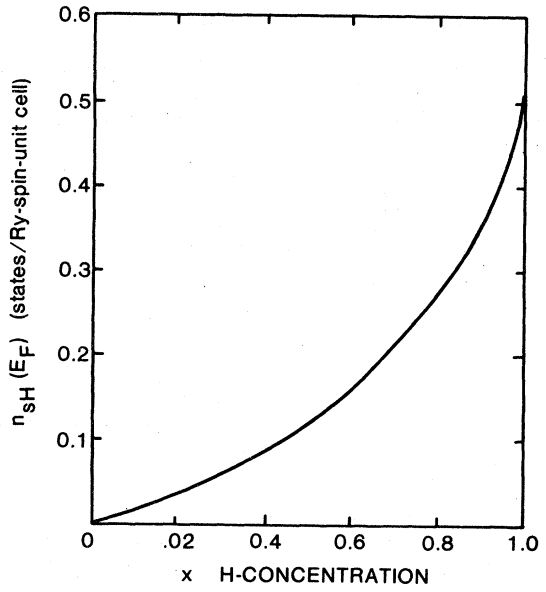

FIG. 5. Hydrogen s-like density of states at the Fermi level plotted vs hydrogen concentration.

the muffin tins. On the other hand, the tight-binding CPA, which we are using here, gives the DOS within the total unit cell rather than the muffin-tin spheres. Due to this constraint we cannot apply Eq. (6) exactly. Hence we will propose an approximate formula derived from the following arguments. Our previous results,[3,4] which are based on the RBA, have shown that $\eta_{Pd} \approx$ constant and that η_H increases with x. Also from the RBA results, a careful evaluation of all terms entering into Eq. (6) reveals that the increase of η_H is almost entirely determined by an increase of the DOS ratio n_{sH}/n_t, with the other quantities varying very slowly with x. We expect this to be true for the CPA results since E_F takes almost the same values as a function of x for both the RBA and the CPA. These observations suggest the following approximate formulas for the electron-phonon interaction of the H and Pd sites, respectively:

$$\eta_H \approx C_H \frac{n_{sH}}{n_t}(E_F); \quad \eta_{Pd} \approx C_{Pd} \frac{n_{dPd}}{n_t}(E_F), \tag{7}$$

where n_{sH} is the hydrogen site s-like DOS, n_{dPd} is the Pd-site d-like DOS, and n_t the total DOS, all evaluated at E_F. The proportionality constants C_H and C_{Pd} are determined from our exact results[3,4] for $x = 1.0$ (stoichiometric case). The values of the DOS at E_F as well as η_H and η_{Pd} found from Eq. (7) are listed in Table III.

We have calculated the electron-phonon coupling constant λ and T_c using the Allen-Dynes equation,[22] neutron-scattering measurements,[23] and μ^* from the Bennemann-Garland[24] formula as explained in Ref. 4. Our CPA results are shown in Table IV, and they are compared with those we found using the RBA.[3,4] We note that in the high-T_c region, $1.0 \leq x \leq 0.8$, λ_{Pd} has a small variation rather than being constant as predicted by the RBA. On the other hand, $\lambda_{H(D)}$ changes by a factor of 2 just as in the RBA calculations. Comparing the CPA and RBA values of λ we find an approximately 10% difference at $x = 0.8$ and less than 1% difference at $x = 0.9$.

The distinction between λ_H and λ_D, shown in Table IV, has been introduced by using the following relationship between the force constants: $k_{Pd\text{-}H} = 1.2\, k_{Pd\text{-}D}$. This has been derived from experiment[23,25] and is sufficient to give a quantitative explanation of the inverse isotope effect as discussed in Refs. 3 and 4, and is now verified from the CPA-derived T_c values of Table IV.

In conclusion, the CPA results strongly support our previous analysis regarding superconductivity in the Pd-H system. The increase of T_c with x is mainly due to the increase of the hydrogen-site electron-phonon interaction η_H, which in turn oc-

TABLE III. Values of the densities of states at E_F and electron-phonon interaction η as a function of hydrogen concentration x.

x	E_F (Ry)	(states/Ry unit-cell spin) n_t	n_{sPd}	n_{pPd}	n_{d_1}	n_{d_2}	n_{sH}	n_{dPd}/n_t	n_{sH}/n_t	(eV/Å^2) η_{Pd}	η_H
1.0	0.642	3.140	0.272	0.450	1.545	0.361	0.512	0.607	0.163	0.865	0.392
0.9	0.633	3.114	0.261	0.408	1.688	0.412	0.346	0.674	0.111	0.960	0.267
0.8	0.620	3.096	0.249	0.347	1.803	0.437	0.261	0.723	0.084	1.030	0.202
0.7	0.610	3.522	0.267	0.311	2.213	0.518	0.214	0.775	0.061	1.104	0.147
0.6	0.600	6.326	0.266	0.275	5.089	0.549	0.148	0.891	0.023	1.272	0.055
0.5	0.596	10.876	0.274	0.255	9.578	0.645	0.124				
0.4	0.593	12.792	0.246	0.228	11.443	0.783	0.092				
0.3	0.591	13.319	0.232	0.191	11.939	0.904	0.054				
0.2	0.588	15.923	0.320	0.246	13.833	1.477	0.047				
0.1	0.585	17.051	0.296	0.198	14.411	2.124	0.021				
0.0	···	17.697	0.242	0.256	13.298	3.901	···				

TABLE IV. Comparison of the electron-phonon coupling constant λ between CPA and RBA. Values of the Coulomb pseudopotential μ^* and T_c for PdD and PdH.

x	λ_{Pd} [a]	λ_D [a]	λ_H [a]	λ_{Pd} [b]	λ_D [b]	λ_H [b]	μ^*	T_c (PdD) Calculated [a]	Experiment [c]	T_c (PdH) Calculated [a]	Experiment [c]
1.0	0.175	0.450	0.369	0.175	0.450	0.369	0.082	10.4	9.8	9.0	8.0
0.9	0.194	0.307	0.251	0.176	0.324	0.268	0.082	5.0	5.4	4.1	3.9
0.8	0.208	0.233	0.190	0.176	0.224	0.179	0.081	2.8	2.4	2.1	1.3

[a] Present results using the CPA.
[b] Results from Ref. 4 using the rigid-band approximation (RBA).
[c] Reference 10.

curs because of the increase with x of the H electronic density of states of s character at E_F.

Using our CPA results for $n_t(x)$ and $\lambda(x)$ of PdH_x, we have also evaluated the coefficient of the electronic specific heat, from the well-known expression

$$\gamma = \tfrac{2}{3}\pi^2 k_B^2 (1+\lambda) n_t(E_F). \tag{8}$$

The results are given in Table V and compared with the measured values of Mackliet *et al.*[7,26] and of Wolf *et al.*[27,28] The agreement is very good. Recent measurements by Wolf and Zimmermann[29] on PdH_x suggest that $\gamma_{PdD} < \gamma_{PdH}$ by almost a factor of 2. This is in direct disagreement with our calculations. Our view has been[4] that due to the very small difference of the lattice constants, the band structures of PdD_x and PdH_x are almost identical. Therefore, $n_t(E_F)$ is the same for both PdD_x and PdH_x. The only difference in γ can be introduced by the different enhancements λ. This difference, however, is small and in the opposite direction to the measurements.[29] According to Wolf and Zimmermann,[29] there is a possibility for an error in their determination of γ_{PdD} due to a shift of the regression range towards higher temperatures which could shift γ_{PdD} to lower values.

Comparison of our DOS results with susceptibility measurements[30] cannot be made accurately. The reason is that the measured susceptibility is a sum of four different terms,[31] only one of which, the Pauli susceptibility, is directly related to the DOS. If we make the assumption that the measured susceptibility is dominated by the Pauli susceptibility, then our calculated $n_t(E_F)$, shown in Fig. 4, are consistent with the measurements. Finally, we wish to point out that the susceptibility measurements[30] do not show any difference between PdD and PdH.

V. CONCLUSIONS

These CPA calculations of the electronic states in nonstoichiometric PdH_x appear to be quite reliable for values of x greater than about 0.6. We believe that our physical model is close to reality in this β-phase region of the PdH_x phase diagram.[32] In the two-phase region which corresponds to lower values of x we expect our results to be less reliable for two reasons. First of all, there should be a great deal of short-range order in the distribution of hydrogen atoms in the crystal and large strain fields which are not accounted for in the CPA theory. Secondly, as one considers smaller values of x, the use of the $PdH_{1.0}$ Slater-Koster parameters as input to the tight-binding CPA becomes increasingly inaccurate. In addition, we note that the Pd atoms undergo relatively large displacements in the α-phase region, as can be seen from the difference in lattice constants between Pd and $PdH_{1.0}$. In the β-phase region the

TABLE V. Calculated and measured coefficient of electronic specific heat γ, calculated electron-phonon coupling constant λ, and total density of states at the Fermi level $n_t(E_F)$, as a function of hydrogen concentration x, for PdH_x.

x	λ	$n_t(E_F)$ (states/Ry spin unit-cell)	γ (mJ/mole °K^2) γ_{calc} [a]	γ_{calc} [b]	γ_{expt} [c]	γ_{expt} [d]
1.0	0.544	3.140	1.68	1.77	•••	•••
0.90	0.445	3.114	1.56	1.86	1.53	1.29
0.80	0.398	3.096	1.50	1.92	1.50	1.48
0.70	0.361	3.522	1.66	2.90	•••	1.40
0.60	0.309	6.326	2.87	•••	2.50	2.00

[a] CPA results
[b] RBA results, Ref. 4.
[c] References 7 and 26.
[d] References 27 and 28.

lattice constant varies[33] by only 2%. Such a small difference in the lattice spacing should not introduce any appreciable change to the DOS at E_F, since E_F falls at a flat region of the DOS.

Calculations for nonstoichiometric PdH_x using the ATA have been applied to study heats of formation[20] and also Fermi surfaces[34] for small values of x. We believe that the CPA approach is conceptually a significantly better way to treat substoichiometric materials than the ATA method. The difficulties experienced in the ATA Fermi surface calculations can be traced to both the problems in studying the α-phase region that we have discussed, and also to the theoretical limitations of the ATA. We are not able to do any detailed comparison with the ATA calculations of Gelatt *et al.*,[20] as in that work they did not present DOS results.

The present calculations lead to the same physical picture that has been proposed previously[3,4] using the rigid-band approximation to explain the superconducting properties of PdH_x. The more rigorous CPA method that we have used here puts these conclusions on much firmer theoretical grounds. It would be useful to do further studies on PdH_x using the full muffin-tin CPA[35] rather than the tight-binding version that we have used here.

ACKNOWLEDGMENTS

We wish to thank E. N. Economou for helpful discussions and L. S. Birks and D. J. Nagel for comments on the manuscript.

[1]P. Soven, Phys. Rev. 156, 809 (1967).
[2]J. S. Faulkner, Phys. Rev. B 13, 2391 (1976).
[3]B. M. Klein, E. N. Economou, and D. A. Papaconstantopoulos, Phys. Rev. Lett. 39, 574 (1977).
[4]D. A. Papaconstantopoulos, B. M. Klein, E. N. Economou, and L. L. Boyer, Phys. Rev. B 17, 141 (1978).
[5]J. C. Slater and G. F. Koster, Phys. Rev. 94, 1498 (1954).
[6]D. E. Eastman, J. K. Cashion, and A. C. Switendick, Phys. Rev. Lett. 27, 35 (1971).
[7]C. A. Mackliet, D. J. Gillespie, and A. I. Schindler, J. Phys. Chem. Solids 37, 379 (1976).
[8]T. Skoskiewicz, Phys. Status Solidi A 11, k123 (1972).
[9]B. Stritzker and W. Buckel, Z. Phys. 257, 1 (1972).
[10]J. E. Schirber and C. J. M. Northrup, Jr., Phys. Rev. B 10, 3818 (1974).
[11]R. J. Miller and C. B. Satterthwaite, Phys. Rev. Lett. 34, 144 (1975).
[12]J. W. D. Connolly, in *Electronic Density of States*, Nat. Bur. Stand. Spec. Publ. No. 323, (U. S. GPO, Washington, D.C., 1971), p. 27.
[13]L. F. Mattheiss, Phys. Rev. B 5, 290 (1972).
[14]J. M. Honig, W. E. Wahnsiedler, and J. O. Dimmock, J. Solid State Chem. 5, 452 (1972).
[15]K. Schwarz, J. Phys. C 8, 809 (1975).
[16]L. F. Mattheiss, Phys. Rev. B 12, 2161 (1975).
[17]A. C. Switendick, Ber. Bunsenges. Phys. Chem. 76, 535 (1972).
[18]Minimization routine was obtained from the Courant Institute of Mathematical Sciences, New York University. Based on M. J. D. Powell, Comput. J. 7, 155 (1964).
[19]J. F. Cornwell, *Group Theory and Electronic Energy Bands in Solids* (North-Holland, Amsterdam, 1969).
[20]C. D. Gelatt, Jr., H. Ehrenreich, and J. A. Weiss, Phys. Rev. B 17, 1940 (1978).
[21]G. D. Gaspari and B. L. Gyorffy, Phys. Rev. Lett. 29 801 (1972).
[22]P. B. Allen and R. C. Dynes, Phys. Rev. B 12, 905 (1975).
[23]J. M. Rowe, J. J. Rush, H. G. Smith, M. Mostoller, and H. E. Flotow, Phys. Rev. Lett. 33, 1297 (1974).
[24]K. H. Bennemann and J. W. Garland, AIP Conf. Proc. 4, 103 (1972).
[25]A. Rahman, K. Skold, C. Pelizzari and S. K. Sinha, Phys. Rev. B 14, 3630 (1976).
[26]C. A. Mackliet and A. I. Schindler, Phys. Rev. 146 , 436 (1966).
[27]M. Zimmermann, G. Wolf, and K. Bohmhamel, Phys. Status Solidi A 31, 511 (1975).
[28]G. Wolf, M. Zimmerman, and K. Bohmhamel, Phys. Status Solidi A 37, 179 (1976).
[29]G. Wolf and M. Zimmerman, Phys. Status Solidi A 37, 485 (1976).
[30]H. C. Jamieson and F. D. Manchester, J. Phys. F 2, 323 (1972); R. J. Miller, T. O. Brun, and C. B. Satterthwaite (unpublished).
[31]K. L. Liu, A. H. MacDonald, and S. H. Vosko, Can. J. Phys. 55, 1991 (1977).
[32]F. A. Lewis, *The Palladium/Hydrogen System* (Academic, New York, 1967).
[33]J. E. Schirber and B. Morosin, Phys. Rev. B 12, 117 (1975).
[34]S. Bessendorf, L. Schwartz, and A. Bansil, Bull. Am. Phys. Soc. 23, 234 (1978).
[35]G. M. Stocks, W. M. Temmerman, and B. L. Gyorffy, Phys. Rev. Lett. 41, 339 (1978).